Proc. of the 2nd European Conference on Electrical Engineering & Computer Science (EECS 2018),
Bern, Switzerland, December 20-22

Extended Kalman Filter Design and Motion Prediction of Ships using Live Automatic Identification System (AIS) Data

Sindre Fossen
Department of ICT and Natural Sciences
NTNU Norwegian University of Science and Technology
Ålesund, Norway
E-mail: sindre@fossen.biz

Thor I. Fossen
Department of Engineering Cybernetics
NTNU Norwegian University of Science and Technology
Trondheim, Norway
E-mail: thor.fossen@ntnu.no

***Abstract*—This paper addresses the problem of ship motion estimation using live data from Automatic Identification Systems (AIS) and extended Kalman filter (EKF) design. AIS data are transmitted from ships globally and a very-high frequency (VHF) AIS receiver picks up the signals as coded ASCII characters in a format specified by the National Marine Electronics Association (NMEA). Hence, the AIS sentences must be decoded using a parser to obtain real-time ship position, course and speed measurements. The state estimates are intended for collision detection and real-time visualization, which are important features of modern decision-support systems.**

The EKF is validated using live AIS data from the Trondheim harbor in Norway and it is demonstrated that the estimator can track ships in real time. It is also demonstrated that the EKF can predict the future motion of ships and different evasive maneuvers were analyzed in a collision avoidance scenario.

***Index Terms*—Kalman filter, state estimation, motion prediction, collision detection, unmanned surface vehicles, ships**

I. Introduction

AIS is a global system, which allows ships to view marine traffic in their area and to be seen by other ships [1]. Vessels are equipped with a dedicated VHF AIS transceiver, which can be used for motion prediction, see Fig. 1. Live AIS data has been used for state estimation by [6] who uses a linear discrete-time Kalman filter. Our approach differs from this work in that a nonlinear kinematic model is used to describe the ship motions [3]. Another difference is how the ship's acceleration and yaw rate are estimated. Since the system model is nonlinear, an EKF is used for state estimation and prediction [4].

The AIS data is transmitted using the UDP protocol. Hence, the EKF must handle delayed measurements, asynchronous communication as well as loss of packets. The EKF runs at a fixed time step and the output is evenly spaced data. Since, the AIS data are transmitted at asynchronous time samples, the EKF is implemented in discrete time using the *predictor-corrector* representation [4].

Game technology is used more and more in decision-support systems for simulation, 3-D visualization and augmented/virtual reality (AR/VR). The human eye requires 30-60 frames per second (FPS) to make pictures appear as a smooth film. This also applies to a pilot who operates an unmanned surface vehicle (USV) using a 3-D visualization system. Hence, the position and course of the AIS ships must be estimated at 30-60 Hz to satisfy human constraints.

In this paper, the following motion prediction and collision detection scenarios are demonstrated:

- Decoding of live asynchronous AIS data using a parser.
- Implementation of an EKF for generation of position, velocity and course for visualization of ship motions in real time at evenly spaced times.
- Motion prediction of AIS ships and online computation of distances between ships (collision detection).
- Motion prediction of interceptor (USV) when approaching targets (AIS ships) and demonstrating how an evasive maneuver can prevent collision.

II. AIS Decoder

Live AIS data for visualization and motion prediction can be obtained by using a VHF antenna. Fig. 1 shows the VHF antenna and AIS decoder in cascade with the motion prediction algorithm.

There are 27 AIS messages with different priority that are transmitted using class A and B transceivers [7]. For ship tracking and motion prediction the position reports of messages 1, 2, 3 and 18 are particularly useful. These messages contain longitude, latitude, speed over ground (SOG), course over ground (COG), yaw rate, true heading etc.

The AIS data are transmitted using the UDP Internet protocol. The coded AIS sentences are ASCII characters as defined by the National Marine Electronics Association format [8]. The bits can be decoded to live ship motion measurements by using the [7] specifications. Several open source codes are available at GitHub (http://www.github.com).

This work was partially funded by the Norwegian Research Council (NTNU AMOS) at the Norwegian University of Science and Technology (grant no. 223254).

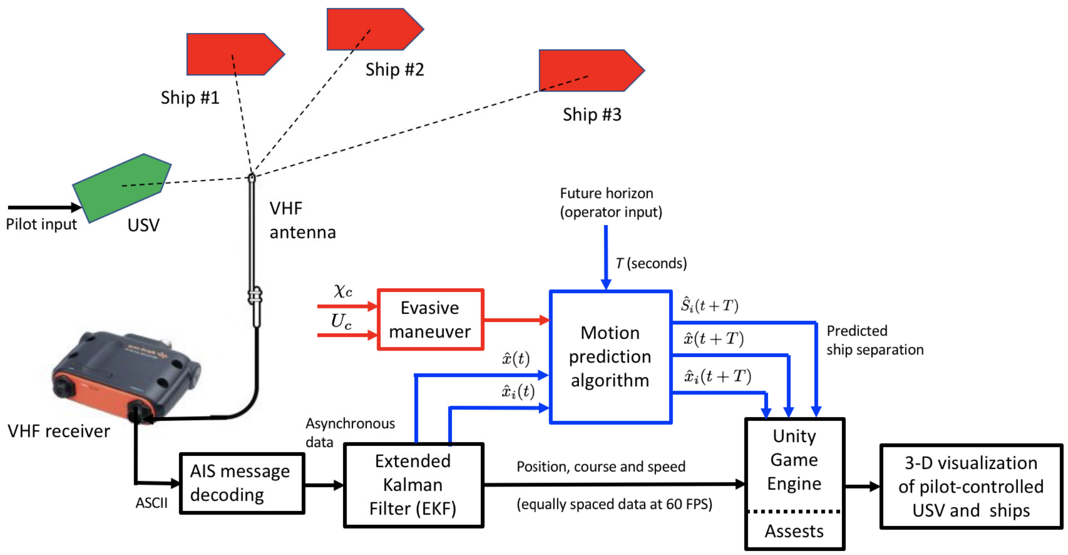

Fig. 1. Decoding of AIS messages and visualization of USV and ships using the Unity Game Engine [10]. The EKF is used to interpolate the asynchronous data for visualization at 60 FPS and to handle UDP packet losses. The future motions (T seconds) including evasive maneuvers are computed using the motion predictor algorithm, which again can be used in a collision detection algorithm.

III. Ship Model

Let the North-East positions and course angle be denoted (x, y) and χ, respectively. Consequently, a ship moving at speed U and course χ is given by [3]:

$$\boxed{\begin{aligned} \dot{x} &= U\cos(\chi) \\ \dot{y} &= U\sin(\chi) \\ \dot{U} &= a \\ \dot{\chi} &= r \end{aligned}} \qquad \begin{aligned} &(1)\\ &(2)\\ &(3)\\ &(4) \end{aligned}$$

The linear acceleration a and course rate r are ship dependent and unknown. If the AIS data are received at a frequency slower than e.g. 0.5 Hz it is recommended to use $a = r = 0$. However, for high-speed craft AIS data are transmitted at a much higher frequency. Hence, it is possible to compute estimates a_c and r_c of a and r, respectively from the AIS measurements. The estimates are filtered to avoid rapid changes:

$$\boxed{\begin{aligned} \dot{a} &= \frac{1}{T_a}\left(\mathrm{sat}(a_c) - a\right) \\ \dot{r} &= \frac{1}{T_r}\left(\mathrm{sat}(r_c) - r\right) \end{aligned}} \qquad \begin{aligned} &(5)\\ &(6) \end{aligned}$$

Here T_a and T_r are user defined time constants. The saturation function $\mathrm{sat}(x)$ ensures that $|x| \leq x_{\max}$, which adds robustness to AIS wildpoints.

Let the last three AIS speed and course measurements at times (t_m, t_{m-1}, t_{m-2}) be denoted $(U_m^{\mathrm{AIS}}, U_{m-1}^{\mathrm{AIS}}, U_{m-2}^{\mathrm{AIS}})$ and $(\chi_m^{\mathrm{AIS}}, \chi_{m-1}^{\mathrm{AIS}}, \chi_{m-2}^{\mathrm{AIS}})$, respectively. Furthermore, let $h_1 = t_m - t_{m-1}$ and $h_2 = t_{m-1} - t_{m-2}$. Unfortunately, the data is not evenly spaced, that is $h_1 \neq h_2$. To deal with asynchronous measurements, a *backward difference approximation* of the first derivative is derived (see the Appendix for details):

$$\boxed{\begin{aligned} a_c &= \frac{(1-\alpha)U_m^{\mathrm{AIS}} + \alpha U_{m-1}^{\mathrm{AIS}} - U_{m-2}^{\mathrm{AIS}}}{(1-\alpha)h_1 + h_2} \\ r_c &= \frac{(1-\alpha)\chi_m^{\mathrm{AIS}} + \alpha \chi_{m-1}^{\mathrm{AIS}} - \chi_{m-2}^{\mathrm{AIS}}}{(1-\alpha)h_1 + h_2} \end{aligned}} \qquad \begin{aligned} &(7)\\ &(8) \end{aligned}$$

where $\alpha = (h_1 + h_2)^2/h_1^2$.

IV. AIS Measurements

The following AIS measurements are used by the EKF:

- SOG and COG corresponding to the states U and χ.
- Longitude l and latitude μ.

Longitude and latitude can be mapped to Cartesian coordinates using the World Geodetic System (WGS-84), which is the standard coordinate system for the Earth.

For local navigation and visualization it is convenient to use a flat Earth approximation based on WGS-84. The procedure is outlined below [2].

A. North-East positions from longitude and latitude (WGS-84)

Assume that the flat Earth coordinate origin is located at longitude and latitude (l_0, μ_0) and define:

$$\Delta l := l - l_0 \tag{9}$$

$$\Delta\mu := \mu - \mu_0 \tag{10}$$

The Earth radius of curvature in the prime vertical R_N and the radius of curvature in the meridian R_M are [9]:

$$R_N = \frac{a}{\sqrt{1 - e^2 \sin^2(\mu_0)}} \tag{11}$$

$$R_M = R_N \frac{1 - e^2}{\sqrt{1 - e^2 \sin^2(\mu_0)}} \tag{12}$$

where $a = 6\,378\,137$ m is the semi-minor axis (equatorial radius) and $e = 0.0818$ is the Earth eccentricity. Small changes in the North and East positions (x, y) are computed as:

$$x = \frac{\Delta\mu}{\text{atan2}(1, R_M)} \tag{13}$$

$$y = \frac{\Delta l}{\text{atan2}(1, R_N \cos(\mu_0))} \tag{14}$$

V. Extended Kalman Filter

The nonlinear system model (1)–(6) can be expressed as:

$$\dot{\mathbf{x}} = \mathbf{f}(\mathbf{x}) + \mathbf{B}\mathbf{u} + \mathbf{w} \tag{15}$$

$$\mathbf{y} = \mathbf{C}\mathbf{x} + \mathbf{e} \tag{16}$$

where $\mathbf{x} = [x, y, U, \chi]^\top$, $\mathbf{u} = [a, r]^\top$, $\mathbf{w}$ and $\mathbf{e}$ are Gaussian process and measurement noise, respectively,

$$\mathbf{f}(\mathbf{x}) = \begin{bmatrix} x_3 \cos(x_4) \\ x_3 \sin(x_4) \\ 0 \\ 0 \end{bmatrix}, \quad \mathbf{B} = \begin{bmatrix} 0 & 0 \\ 0 & 0 \\ 1 & 0 \\ 0 & 1 \end{bmatrix} \tag{17}$$

and $\boldsymbol{C} = \boldsymbol{I}_4$. The EKF makes use of the linearized expression:

$$\mathbf{A} = \frac{\partial \mathbf{f}(\mathbf{x})}{\partial \mathbf{x}} = \begin{bmatrix} 0 & 0 & \cos(x_4) & -x_3 \sin(x_4) \\ 0 & 0 & \sin(x_4) & x_3 \cos(x_4) \\ 0 & 0 & 0 & 0 \\ 0 & 0 & 0 & 0 \end{bmatrix} \tag{18}$$

The discrete-time EKF then becomes [4]:

Kalman gain:

$$\boldsymbol{K}(k) = \hat{\boldsymbol{P}}^-(k)\boldsymbol{C}^\top \left(\boldsymbol{C}\hat{\boldsymbol{P}}^-(k)\boldsymbol{C}^\top + \boldsymbol{R}\right)^{-1} \tag{19}$$

Corrector:

$$\hat{\boldsymbol{x}}^+(k) = \hat{\boldsymbol{x}}^-(k) + \boldsymbol{K}(k)\left(\boldsymbol{y}(k) - \boldsymbol{C}\hat{\boldsymbol{x}}^-(k)\right) \tag{20}$$

$$\begin{aligned} \hat{\boldsymbol{P}}^+(k) = {} & (\boldsymbol{I}_4 - \boldsymbol{K}(k)\boldsymbol{C})\hat{\boldsymbol{P}}^-(k)\,(\boldsymbol{I}_4 - \boldsymbol{K}(k)\boldsymbol{C})^\top \\ & + \boldsymbol{K}(k)\boldsymbol{R}\boldsymbol{K}^\top(k) \end{aligned} \tag{21}$$

Predictor:

$$\hat{\boldsymbol{x}}^-(k+1) = \hat{\boldsymbol{x}}^+(k) + h\boldsymbol{f}(\hat{\boldsymbol{x}}^+(k)) + h\boldsymbol{B}\boldsymbol{u}(k) \tag{22}$$

$$\hat{\boldsymbol{P}}^-(k+1) = \boldsymbol{\Phi}(k)\hat{\boldsymbol{P}}^+(k)\boldsymbol{\Phi}^\top(k) + \boldsymbol{Q} \tag{23}$$

where $\hat{\boldsymbol{x}}^-(0) = \boldsymbol{x}(0)$, $\hat{\boldsymbol{P}}^-(0) = \boldsymbol{P}(0)$, h is the sampling time, $\boldsymbol{Q} = \boldsymbol{Q}^\top > 0$ and $\boldsymbol{R} = \boldsymbol{R}^\top > 0$ are the process covariance and measurement matrices, respectively,

$$\boldsymbol{\Phi}_k = \boldsymbol{I}_4 + h\boldsymbol{A} + \frac{1}{2}h^2\boldsymbol{A}^2 +, ..., + \frac{1}{n!}h^n\boldsymbol{A}^n \tag{24}$$

Let $\boldsymbol{\varepsilon}(k) = \boldsymbol{y}(k) - \boldsymbol{C}\hat{\boldsymbol{x}}^-(k)$ denote the estimation error in (20). When implementing the corrector, it is necessary to map the course angle estimation error $\varepsilon_4(k) = \chi(k) - \hat{\chi}^-(k)$ to the interval $[-\pi, \pi)$. This is referred to as the *smallest signed angle*, which can be computed using the function:

$$\text{ssa}(x) = \text{mod}(x + \pi, 2\pi) - \pi \tag{25}$$

VI. Ship Motion Prediction

The ship model (1)–(6) can be used to predict the ship motions from the last AIS measurement at time t_0 to $t = t_0 + T$ where T is final time, see Fig. 1. Let h be the sampling time. Hence, the discrete-time predictor for the interceptor (USV) becomes:

USV:

$$x(k+1) = x(k) + hU(k)\cos\left(\chi(k)\right) \tag{26}$$

$$y(k+1) = y(k) + hU(k)\sin\left(\chi(k)\right) \tag{27}$$

$$U(k+1) = U(k) + ha(k) \tag{28}$$

$$\chi(k+1) = \chi(k) + hr(k) \tag{29}$$

$$a(k+1) = a(k) + \frac{h}{T_a}\left(\text{sat}(a_c) - a(k)\right) \tag{30}$$

$$r(k+1) = r(k) + \frac{h}{T_r}\left(\text{sat}(r_c) - r(k)\right) \tag{31}$$

where $x(0) = x(t_0), y(0) = y(t_0), U(0) = U(t_0)$, $\chi(0) = \chi(t_0)$, $a(0) = a(t_0)$ and $r(0) = r(t_0)$. The target (AIS) ships motion predictors are $(i = 1, 2, ..., N)$:

AIS ship #i:

$$x_i(k+1) = x_i(k) + hU_i(k)\cos\left(\chi_i(k)\right) \tag{32}$$

$$y_i(k+1) = y_i(k) + hU_i(k)\sin\left(\chi_i(k)\right) \tag{33}$$

$$U_i(k+1) = U_i(k) + ha_i(k) \tag{34}$$

$$\chi_i(k+1) = \chi_i(k) + hr_i(k) \tag{35}$$

$$a_i(k+1) = a_i(k) + \frac{h}{T_a}\left(\text{sat}(a_{c_i}) - a_i(k)\right) \tag{36}$$

$$r_i(k+1) = r_i(k) + \frac{h}{T_r}\left(\text{sat}(r_{c_i}) - r_i(k)\right) \tag{37}$$

where $x_i(0) = x_i(t_0), y_i(0) = y_i(t_0), U_i(0) = U_i(t_0)$, $\chi_i(0) = \chi_i(t_0)$, $a_i(0) = a_i(t_0)$ and $r_i(0) = r_i(t_0)$.

A. Collision detection

The motion predictors can be used to identify possible collisions by computing the instantaneous separation between the ships. Let the the coordinate origin of the ships be located midships on the centerline. Furthermore, let (x, y) denote the *interceptor* (USV) position and (x_i, y_i) where $i = 1, 2, \cdots, N$ be the target (AIS) ship positions. The relative position errors between the USV and AIS ship $\#i$ then become:

$$e_{x_i}(k) = x(k) - x_i(k) \tag{38}$$

$$e_{y_i}(k) = y(k) - y_i(k) \tag{39}$$

and the minimum separation $S(k)$ between the USV and AIS ships are:

$$S(k) = \min_i \sqrt{e_{x_i}^2(k) + e_{y_i}^2(k)} \tag{40}$$

Fig. 2. The MS Trondheimsjord II is high-speed catamaran for passenger transport. Length 24.5 m, beam 8.0 m and maximum speed 16.5 m/s (32 knots).

B. Predictor for evasive maneuvers

If the minimum separation (40) is to small, the USV speed and course (28)–(29) can be modified to include the effect of an evasive USV maneuver. A typical collision avoidance maneuver can be specified in terms of a speed command U_c and a course angle command χ_c, for instance:

- Reduce the intercepter speed $U(0)$ by 50 %:
  $\Longrightarrow \;\; U_c = 0.5\, U(0)$
- Align the interceptor course $\chi(0)$ to the target course:
  $\Longrightarrow \;\; \chi_c = \chi_i(0)$

The next step is to replace (28)–(29) with the closed-loop speed and course dynamics, typically first-order systems, such that:

$$\boxed{\begin{aligned} x(k+1) &= x(k) + hU(k)\cos\left(\chi(k)\right) && (41)\\ y(k+1) &= y(k) + hU(k)\sin\left(\chi(k)\right) && (42)\\ U(k+1) &= U(k) + \frac{h}{T_{\text{speed}}}\left(U_c - U(k)\right) && (43)\\ \chi(k+1) &= \chi(k) + \frac{h}{T_{\text{course}}}\,\text{ssa}\left(\chi_c - \chi(k)\right) && (44) \end{aligned}}$$

where $\text{ssa}(\cdot)$ is the *smallest signed angle* given by (25), $U(0) = U(t_0)$ and $\chi(0) = \chi(t_0)$. The time needed to perform the maneuver is specified by the user inputs T_{speed} and T_{course}.

VII. Experimental Validation

This section describes two motion prediction scenarios using live decoded AIS data for a ship operating in the Trondheim fjord, Norway.

- *Case 1 (Ship Motion Prediction):* Live asynchronous AIS data processed by the EKF and used for motion prediction.
- *Case 2 (USV Evasive Maneuver)* Ship motion prediction for a real ship when a simulated USV approaches the ship and performs an evasive maneuver.

The ship motion prediction algorithm and visualization of live AIS ships can be used to present decision makers and pilots with coherent information to make timely and informed decisions.

As the amount of sensor data increase, it becomes more and more difficult for human operators to achieve situational awareness [5]. Consequently, an automated process, which estimate and project situations using algorithms is of great advantage. This is refereed to as *automated situational assessment* and the presented cases below illustrates how this can be achieved.

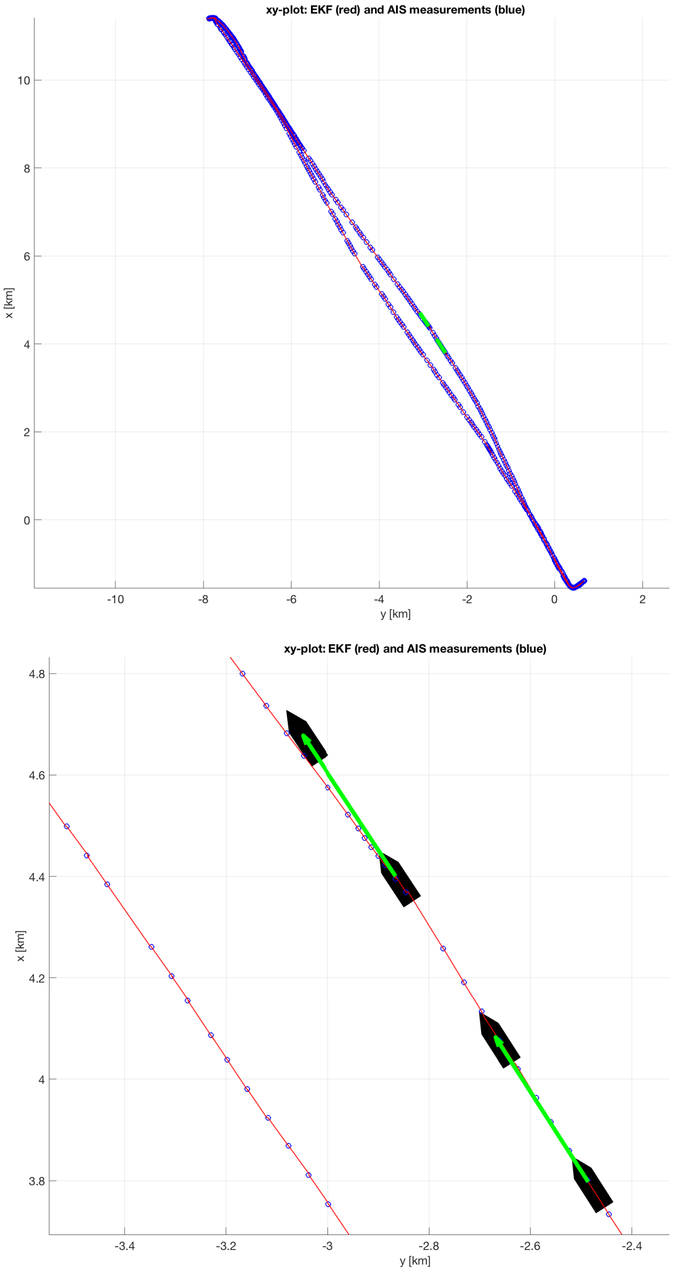

Fig. 3. The upper plot shows the path of MS Trondheimfjord II when crossing the fjord. The lower zoomed plot shows the predicted ship motions at two different locations (black ships) for a future horizon of 30 seconds (green arrows).

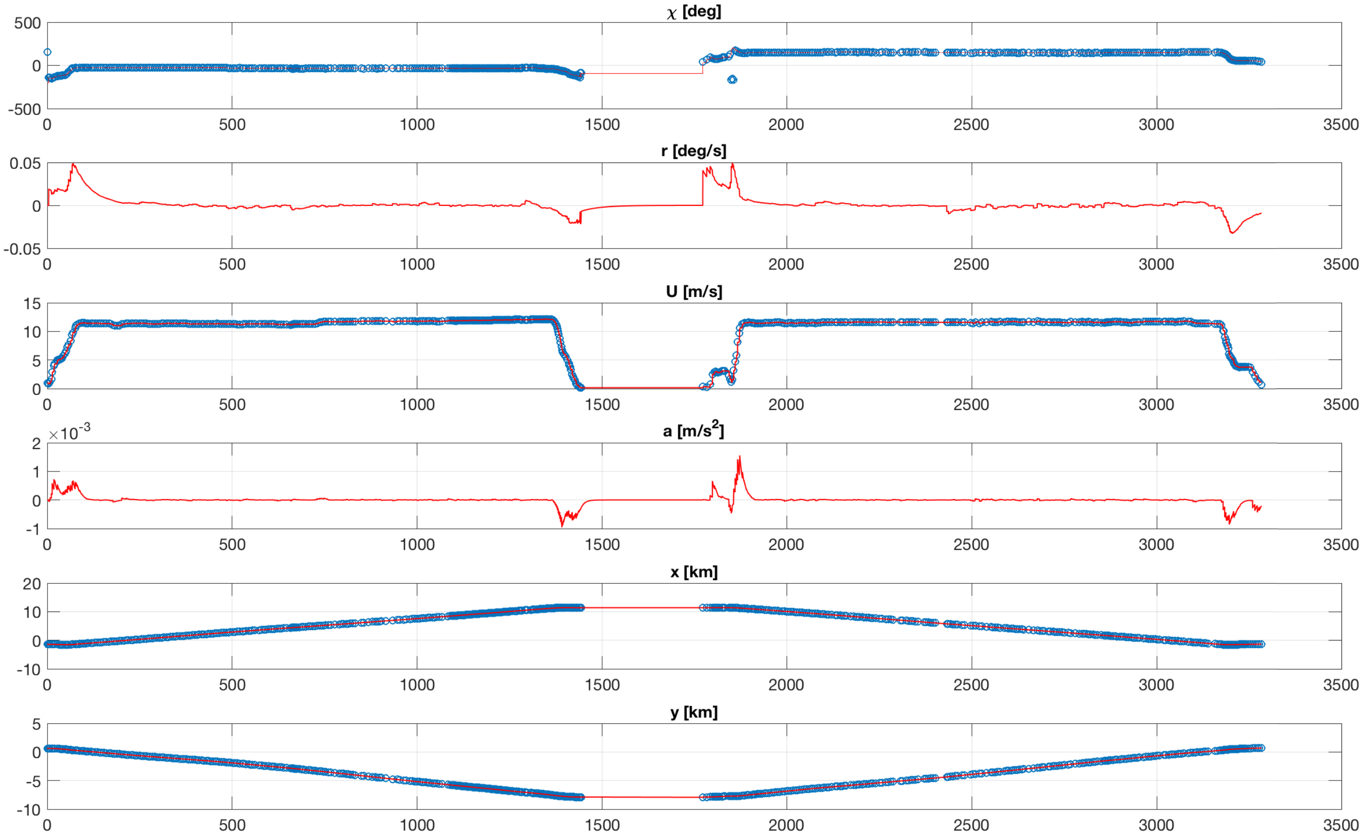

Fig. 4. Estimated states (red) and AIS measurements (blue circles) as a function of time when crossing the fjord back and forth.

Parameters: The EKF is implemented at 50 Hz with $\hat{\boldsymbol{P}}^{-}(0) = 0.1\boldsymbol{I}_4$, $\boldsymbol{Q} = \mathrm{diag}(0.01, 0.01, 0.1, 0.1)$ and $\boldsymbol{R} = \mathrm{diag}(0.001, 0.001, 0.001, 0.01)$. The initial states were chosen as $\hat{\boldsymbol{x}}^{-}(0) = [x(0), y(0), U(0), \chi(0)]^{\top}$, while the time constants were chosen as $T_a = 10$ s and $T_r = 50$ s.

Case 1: Ship Motion Prediction

AIS data for MS Trondheimsfjord II (see Fig. 2) is used to demonstrate ship motion prediction. The asynchronous AIS data are processed by the EKF to obtain equally spaced data at 50 Hz. Fig. 3 shows the path when crossing the Trondheim fjord and Fig. 4 shows the corresponding state estimates. The ship motions are predicted at two different locations with a 30 seconds horizon using (26)–(31).

Fig. 7 shows how the predicted path can be visualized in a situational awareness system using a game engine.

Case 2: USV Evasive Maneuver

The second case study shows an USV that is approaching the MS Trondheimsfjord II from East. The ship and USV motions are predicted using a 60 s future horizon. The USV speed is 10 m/s and the course is -90 deg, see Fig. 6. In order to increase the minimum separation of the USV and the ship, an evasive maneuver as described in Section VI-B is implemented using the motion predictor (41)–(44). Fig. 6 verifies that USV course aligns to the ship course as expected and that the USV speed is reduced from 10 m/s to 5 m/s during the turn. Fig. 5 shows that the minimum separation between the approaching USV and the ship is increased from 126.6 m to 201.0 m by the evasive maneuver.

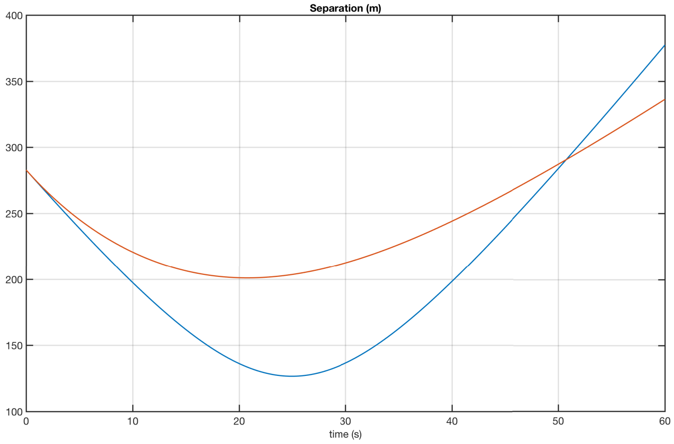

Fig. 5. Minimum separation between an USV approaching MS Trondheimjord II from the East (blue) and when performing an evasive maneuver (red). The minimum distance increases from 126.6 m to 201.0 m.

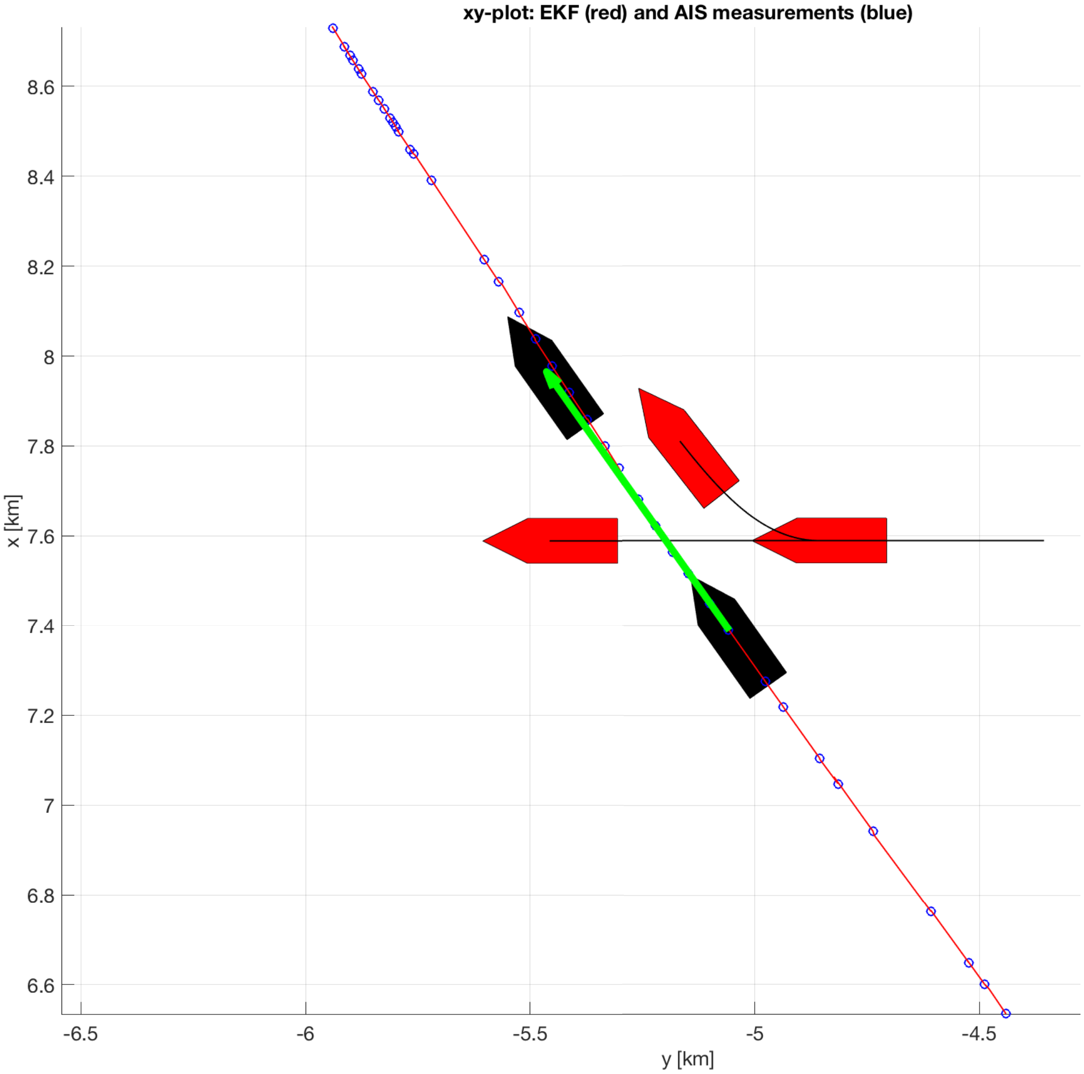

Fig. 6. An USV approaches MS Trondheimsfjord II from the East. The ship and USV motions are predicted in 60 s to show the effect of an evasive maneuver.

VIII. Conclusions

This paper has addressed the problem of ship motion estimation using live data from Automatic Identification Systems (AIS). The sensor data has been processed by an extended Kalman filter (EKF) in order to deal with asynchronous measurements, UDP packet losses and measurement noise. The AIS sentences were decoded using a parser to obtain real-time ship position, course and speed measurements. It has been demonstrated that the state estimates can be used for motion prediction, collision detection and analyses of evasive maneuvers, which are important features of ship decision-support systems.

Finally, the EKF was validated using live AIS data from the Trondheim harbor in Norway and it was demonstrated that the estimator can track ships in real time. It was also demonstrated that the EKF can predict the future motion of ships and an evasive maneuver was analyzed in order to avoid collision.

Acknowledgments

The authors are grateful to Rambøll (www.ramboll.no) and Trondheim municipality for permission to use their 3-D model and GIS data.

Appendix

The backward difference approximation of the first derivative for non-evenly spaced data at times t_k, t_{k-1} and t_{k-2} is derived by using the Taylor-series expansions:

$$F(k-1) = F(k) - h_1 F'(k) + \frac{1}{2} h_1^2 F''(k) + O(h_1^3) \tag{45}$$

$$\begin{aligned} F(k-2) &= F(k) - (h_1 + h_2) F'(k) + \frac{1}{2}(h_1 + h_2)^2 F''(k) \\ &\quad + O((h_1 + h_2)^3) \end{aligned} \tag{46}$$

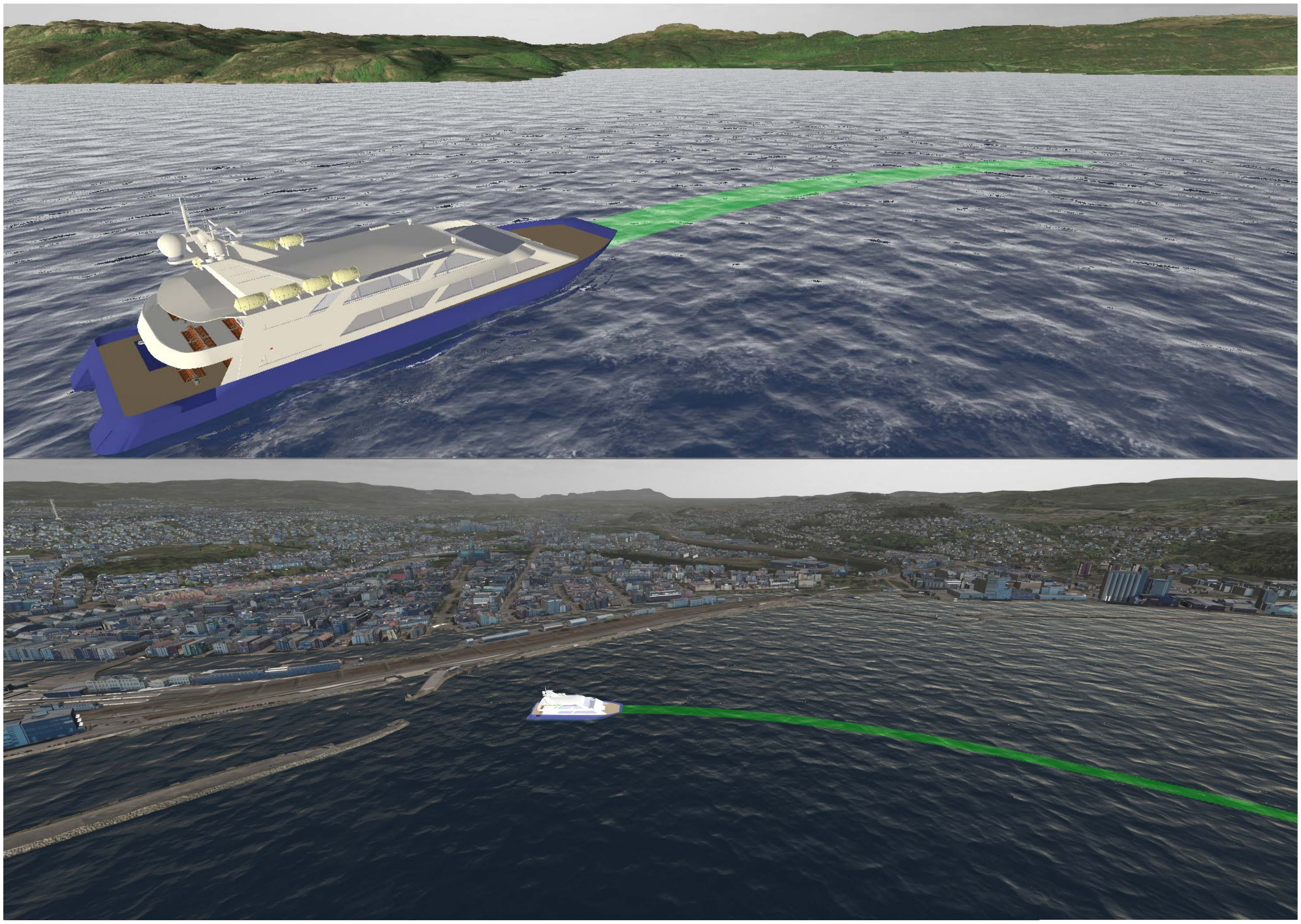

Fig. 7. 3-Disualization of a catamaran passenger boat in the Trondheim fjord using the Unity game engine [10], and the Hydroform Ocean System and Terraland plugins from the Unity Asset Store (http://assetstore.unity.com). The green arrow shows the predicted path of the vessel.

where $h_1 = t_k - t_{k-1}$ and $h_2 = t_{k-1} - t_{k-2}$. Multiplying (45) with

$$\alpha = \frac{(h_1 + h_2)^2}{h_1^2} \tag{47}$$

and subtracting (46) from (45) makes $F''(k)$ vanish. Hence, the error will be of order $O((h_1 + h_2)^3)$. This gives

$$\alpha F(k-1) - F(k-2) = (\alpha-1)F(k) + (-(\alpha-1)h_1 + h_2)\, F'(k) \tag{48}$$

Solving for $F'(k)$, finally gives

$$\boxed{F'(k) = \frac{(1-\alpha)F(k) + \alpha F(k-1) - F(k-2)}{(1-\alpha)h_1 + h_2}} \tag{49}$$

References

[1] Automatic Identification System. Wikipedia. Online; accessed 2018-07-15. URL: https://en.wikipedia.org/wiki/Automatic_identification_system.

[2] J. A. Farrell. “Aided Navigation: GPS with High Rate Sensors”, McGraw-Hill, 2008.

[3] T. I. Fossen. “Handbook of Marine Craft Hydrodynamics and Motion Control”, John Wiley & Sons, Chichester, UK, 2011.

[4] A. Gelb. “Applied Optimal Estimation”, MIT Press, 1974.

[5] J. Holsopple, M. Sudit, M. Nusinov, D. F. Liu, H. Du and S. J. Yang. Enhancing Situation Awareness via Automated Situation Assessment, “IEEE Communications Magazine”, 48(3):146-152, 2010.

[6] K. Jaskolski. Automatic Identification System (AIS) Dynamic Data Estimation based on Discrete Kalman Filter (KF) Algorithm. “Scientific Journal of Polish Naval Academy”, 211(4):7187, 2017.

[7] US Coast Guard Navigation Centre. Online; accessed 2018-08-15. URL: https://www.navcen.uscg.gov/?pageName=AISMessages.

[8] NMEA Standard. Online; accessed 2018-08-15. URL: https://www.nmea.org/content/nmeastandards/nmea0183v410.asp

[9] B. L. Stevens and F. L. Lewis. “Aircraft Control and Simulation”, 2nd Ed., John Wiley & Sons, New York, 2003.

[10] Unity. “The Unity Game Engine”. Online; accessed 2018-07-15. URL: https://unity3d.com